Electrochimica Acta 113 (2013) 570–574

Contents lists available at ScienceDirect

Electrochimica Acta

journal homepage: www.elsevier.com/locate/electacta

Hole conductivity and acceptor density of p-type $CuGaO_2$ nanoparticles determined by impedance spectroscopy: The effect of Mg doping

Isaac Herraiz-Cardona [a], Francisco Fabregat-Santiago [a], Adèle Renaud [b,c], Beatriz Julián-López [d], Fabrice Odobel [a,b], Laurent Cario [c], Stéphane Jobic [c], Sixto Giménez [a,*]

[a] Photovoltaics and Optoelectronic Devices Group, Departament de Física, Universitat Jaume I, 12071 Castelló, Spain
[b] CEISAM, Université de Nantes, CNRS, UMR 6230, 2 rue de la Houssinière, 44322 Nantes Cédex 03, France
[c] Institut des Matériaux Jean Rouxel, Université de Nantes, CNRS, 2 rue de la Houssinière, 44322 Nantes Cédex 03, France
[d] Departament de Química Inorgánica y Orgánica, Universitat Jaume I, 12071 Castelló, Spain

ARTICLE INFO

Article history:
Received 19 August 2013
Received in revised form
19 September 2013
Accepted 21 September 2013
Available online xxx

Keywords:
Delafossite
Impedance spectroscopy
Hole conductivity
Capacitance
Electrochemistry

ABSTRACT

Delafossite materials like $CuGaO_2$ have appeared as promising p-type semiconductor materials for their exploitation in tandem dye sensitized solar cells and water splitting photoelectrochemical cells. However, the intrinsic electronic properties of this material once nanostructured have not been extensively studied and fundamental knowledge is required in order to further develop photovoltaic and photoelectrochemical devices. In the present study, we report the main electrical properties of $CuGaO_2$ nanoparticles and evaluate the effect of Mg doping. We determine for the first time the hole conductivity of mesoporous $CuGaO_2$ using impedance spectroscopy, extracting values ranging from 1 to $10 \times S\,cm^{-1}$ in the interval of applied bias tested. We show that after Mg doping, the optical bandgap is red-shifted 0.15 eV and the conductivity increased one order of magnitude, indicating real p-type doping of the materials. Furthermore, after Mg doping the capacitance showed a Mott–Schottky behaviour reflecting the band bending of the semiconductor. In these conditions, the estimated acceptor density and the flat band potential were $N_A = 10^{19}\,cm^{-3}$ and $V_{FB} = 0.23\,V$ vs Ag/Ag^+, respectively. When the material is not intentionally doped, the measured capacitance corresponds to the double layer capacitance, since the semiconductor is fully depleted in the testing conditions.

1. Introduction

The development of nanostructured p-type semiconductor materials as hole conductors in hybrid photovoltaic and photoelectrochemical devices has received significant attention in the last years, mainly driven by the interest to integrate these materials in hybrid photovoltaic [1] and photoelectrochemical devices [2]. Particularly, materials like NiO have been extensively and almost exclusively studied in the field of p-type dye solar cells [3–6], due to the existing wide experience on the preparation of porous films for the development of electrochromic devices [6]. Additionally, NiO has also been studied as an active hydrogen evolving catalyst in water splitting cells, since Ni appears at the top positions in the Trassatti diagram for hydrogen evolution catalysts [7–9]. On the other hand, p-type Cu_2O has demonstrated promising performance as photocathode in water splitting solar cells, once the severe limitations related to its stability in aqueous environment have been overcome by the addition of protective layers [10–14].

Delafossite $CuGaO_2$ has emerged as a promising p-type material for anodic applications and due to its large bandgap (~3.6 eV), it also appears very attractive as transparent conductive oxide [15]. Moreover, it shows significant synthetic versatility, which entails tailoring its morphological, optical and electronic properties [16]. $CuGaO_2$ has demonstrated interesting photovoltaic properties as photocathode in dye solar cells [17,18] and promising photocatalytic properties to reduce CO_2 to CO [19]. However, it has been recognized that an improved understanding of its fundamental properties is mandatory in order to enhance the current performances achieved [19]. The aim of the present study is to provide a detailed picture of the fundamental electrical properties of this material to have a clear perspective of its functionalities and potential. Additionally, this information will be useful for the design of relevant synthetic guidelines to optimize its performance.

* Corresponding author. Tel.: +34 964387554; fax: +34 964729218.
E-mail address: sjulia@uji.es (S. Giménez).

0013-4686/$ – see front matter © 2013 Elsevier Ltd. All rights reserved.
http://dx.doi.org/10.1016/j.electacta.2013.09.129

We have employed Electrochemical Impedance Spectroscopy (EIS) to extract the most important electronic parameters of this system. EIS entails the frequency analysis of the AC response of a device and it is widely applied in a broad class of material systems and devices, including inorganic, organic and biological systems [20]. The main advantage of this technique relies on the ability to resolve processes with different characteristic time scales with a single measurement, provided that the physical model employed to interpret the experimental results conveys the fundamental processes of interest. In our case we have needed to use a transmission line based model to describe the porous structure of $CuGaO_2$ what allowed to distinguish between charge transport, recombination and accumulation characteristics of the delafossite films.

2. Experimental method

$CuGaO_2$-P123 and $CuGaO_2$:1%Mg materials were synthesized in hydrothermal conditions based on the method developed by Srinivasan et al. with slight modifications [21]. Namely, an aqueous solution of copper, gallium and magnesium nitrates (introduced in stochiometric amounts) containing Pluronic P123 surfactant and NaOH (pH = 5.15) was poured in a 30 ml teflon bomb filled at 70%. The bomb was sealed in an autoclave and heated at 190 °C for 56 h. The as-synthesized samples were then successively washed with liquid ammonia, nitric acid and distilled water to remove any possible traces of Cu_2O, CuO or Cu. The materials were characterized by powder X-ray diffraction on a D8 Brucker diffractometer equipped with a front germanium monochromator (Cu-K-L3 radiation) and a LynxEye PSD detector (Bragg–Brentano geometry). Scanning electron microscopy image were collected on a JEOL7600F apparatus. Brunauer–Emmett–Teller (BET) analyses were done in a micrometrics ASAP 2010BET. The transmittance and diffuse reflectance spectra of the photoelectrodes ($CuGaO_2$ and $CuGaO_2$:1%Mg materials deposited on an FTO-coated glass substrates ((Pilkignton TEC8, 8 Ω cm^2) were recorded between 200 and 800 nm by a Cary 5000 UV–VIS Varian spectrophotometer. An integrating sphere was used for the diffuse reflectance measurements and the absorbance was calculated as: $A = -\log(T+R)$. The absorption coefficient (α) was estimated by $A = \alpha l$, where l is the thickness of the electrode. The direct optical bandgap could be estimated by the Tauc plot, $r = 1/2$ [22].

Cyclic voltammetry, steady-state current density voltage (j–V) and Electrochemical Impedance Spectroscopy (EIS) were carried out using a FRA equipped PGSTAT-30 from Metrohm Autolab. For EIS measurements, the selected frequency range was 10^6–5×10^{-2} Hz, and the amplitude of the AC signal was 20 mV. A three-electrode configuration was used, where the FTO/$CuGaO_2$ electrode was connected to the working electrode, a Pt mesh was connected to the counterelectrode and a non-aqueous Ag/Ag^+ electrode was used as the reference electrode. 0.1 M tetrabutylammonium perchlorate in acetonitrile was used as electrolyte. In order to minimize the effect of the FTO substrate, the exposed FTO surface, not covered by $CuGaO_2$ was passivated by a non-conductive resine, which showed to be stable with the electrolyte. Cyclic voltammetry measurements were carried out at 50 mV s^{-1}. The electrodes were illuminated using a 300 W Xe lamp. The light intensity was adjusted with a thermopile to 100 mW/cm^2, with illumination through the substrate.

3. Results and discussion

The $CuGaO_2$ films were deposited on FTO substrates by screen printing and subsequently heated at 400 °C in Ar atmosphere for 30 min. SEM examination reveals that delafossite films appear as mesoporous layers composed of individual nanoplatelets with approximately 5 nm thick and 100–400 nm wide (Figure SI1). The surface area of the scrapped samples determined by BET was 22 m^2/g and the thickness of the electrode determined by SEM was approximately 4 μm. Mg doping does not introduce significant differences on the morphological properties of the films, although higher surface area was measured by BET, 38 m^2/g.

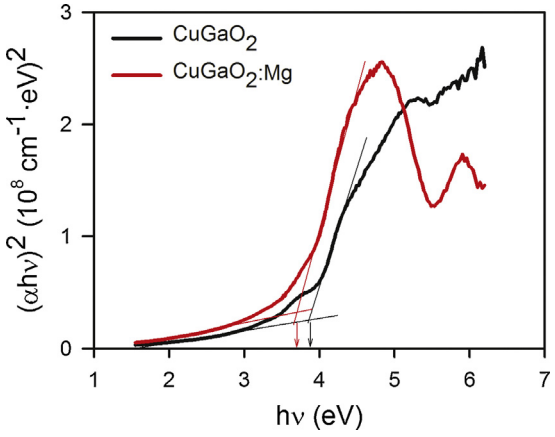

Fig. 1. Tauc plots of the direct bandgap transition for undoped and Mg-doped $CuGaO_2$. The calculations of the bandgaps are indicated by the tangent lines and the arrows.

The optical properties of the material with and without Mg doping are compiled in Fig. 1. We show the Tauc plot for direct bandgap transition extracted from transmittance and reflectance measurements. The direct bandgap obtained for $CuGaO_2$ (3.91 eV) is in reasonable good agreement with those reported by Srinivasan et al. (3.7–3.8 eV) [16], and by Ueda et al. (3.6 eV) [15], and higher compared to the photoelectrochemical measurements carried out by Benko et al. (2.7 eV) [23]. Bandgap anomalies have been reported for delafossite materials, related to a large disparity between the fundamental gap and the apparent optical gap, which is responsible for the bipolar dopability of these materials [24]. On the other hand, Mg doping leads to a slight red-shift of the absorption onset (~0.15 eV), and the obtained direct bandgap is $E_g = 3.76$ eV.

Fig. 2a shows the cyclic voltammograms of the undoped and Mg doped $CuGaO_2$ films. It is clear that Mg doping leads to a more capacitive material as showed by the hysteretic behaviour of the j–V curves. Due to the large bandgap of these materials and the blocking nature of the electrolyte employed in the present study, the dark and illuminated j–V curves are very similar. Fig. 2b shows the potentiostatic current transients after illumination of the sample at −1.2 V vs Ag/Ag^+, clearly reflecting the p-type behaviour of the electrodes (negative photocurrents) and the higher photocurrent measured for the Mg doped material. In these experimental conditions, we did not observe either anodic or cathodic spikes, and consequently charge transfer through surface states can be safely ruled out [1].

Further mechanistic information about the carried dynamics of these materials was extracted from impedance spectroscopy. Potentiostatic frequency scans were carried out at different voltages in the dark and the individual spectra were fitted to a consistent physical model. Figure SI2 shows representative Nyquist plots for a $CuGaO_2$ sample obtained at different applied voltages. The high frequency region of these plots indicates some diffusive contribution (straight line with 45° slope), which depending on the applied voltage appears convoluted with an arc. Since we used a blocking electrolyte for these experiments, the low frequency

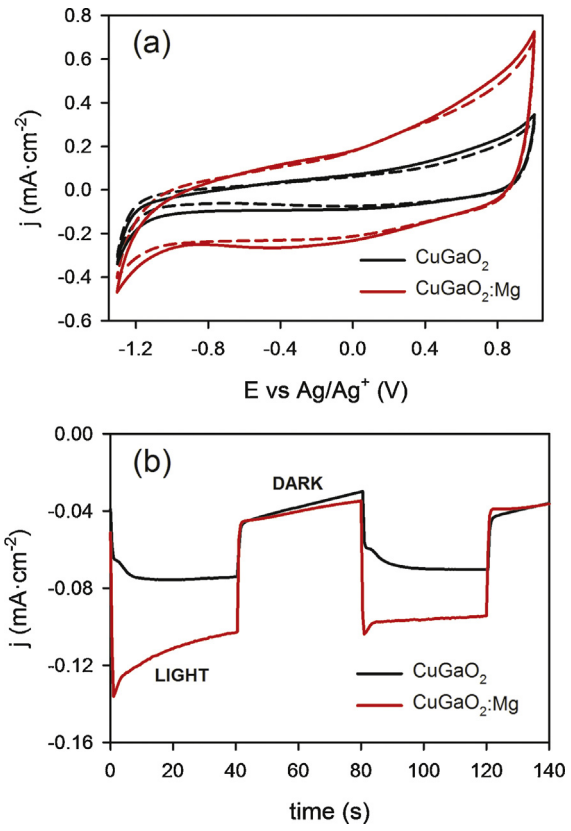

Fig. 2. (a) j–V curves of undoped and Mg doped $CuGaO_2$ in the dark (dashed lines) and under illumination (solid lines). Scan rate was 50 mV s^{-1} (b) potentiostatic current transients obtained for $CuGaO_2$ and $CuGaO_2$:Mg at $V = -1.2$ V vs Ag/Ag^+.

region is dominated by the capacitive behaviour of the electrodes (almost straight vertical line in the Nyquist plots). In order to assess the stability of the samples during the dynamic characterization, cyclic voltammetry curves in the dark and under illumination before and after the impedance spectroscopy measurements were carried out. Figure SI3 shows that the stability of the tested samples was excellent.

In order to model the electrochemical behaviour of the electrodes, we considered a sound physical model, which can be translated into the equivalent circuit depicted in Fig. 3a. In this model, R_s accounts for the series resistance of the electrochemical cell, which includes the contribution of the contact, connection wires, etc., R_{TCO} conveys the information of the charge transfer resistance at the FTO/$CuGaO_2$ interface, C_{TCO} models the capacitance of the FTO/solution interface and T_L is an extended element, accounting for the carrier transport (r_t) through the mesoporous film coupled to charge transfer to the solution (r_{ct}), C_0 is the capacitance at the $CuGaO_2$/solution interface, Fig. 3b. The use of transmission line elements to describe the coupled transport and charge transfer to the solution is well documented in the literature for similar mesoporous systems, like TiO_2 [20,25–27], polypyrrole films [28], etc.

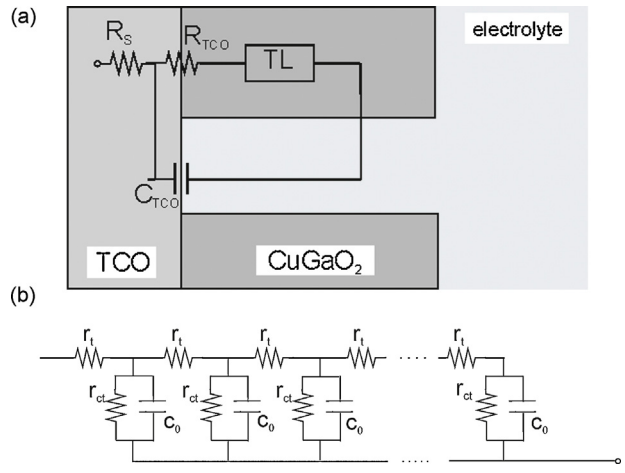

Fig. 3. (a) Equivalent circuit employed to fit the impedance spectra of $CuGaO_2$ samples. (b) Description of the transmission line element (T_L) including a transport resistance (r_t), a recombination or charge transfer resistance (r_{ct}) and a capacitance (C_0).

From fitting the experimental spectra to this model, we could extract information related to the most relevant electronic parameters for the operation of these materials. For example, the transport resistance (r_t) provides information about the film conductivity through the expression:

$$\sigma = \frac{L}{R_t A(1-p)} \quad (1)$$

where L is the film thickness (4 μm from the SEM examination, Figure SI1), A is the geometrical area of the specimens (0.25 cm^2) and p is the porosity of the film ($p = 0.5$ was taken as a first approximation from SEM and BET measurements. The results are showed in Fig. 4a. As expected for p-type semiconductors, the film conductivity increases for both materials with applied bias, as the Fermi level approaches the valence band of the semiconductor (hole conductivity). On the other hand, the conductivity is one order of magnitude higher for the Mg doped material, with values ranging 1–10 μS cm^{-1} in the interval of applied bias tested. These values are considerably lower compared to 20 mS cm^{-1} and 63 mS cm^{-1} reported for undoped $CuGaO_2$ prepared by thermal Pulsed Laser Deposition and co-evaporation of Cu and Ga respectively [15,29]. In any case, to the best of the authors' knowledge, this is the first time that hole conductivities are estimated by impedance spectroscopy using the transmission line extended element for nanostructured p-type semiconductors.

The capacitance of the semiconductor (C_0) is plotted in Fig. 4b. This capacitance conveys the information of the interface $CuGaO_2$/solution and for both the undoped and Mg doped $CuGaO_2$, it increases with applied potential. However, the origin of this capacitance is believed to be different for both materials as discussed below. In order to evaluate the physical origin of this capacitance, we assessed different possibilities: i.e., a dielectric capacitance, a chemical capacitance or a double layer capacitance. For the undoped material, the Mott–Schottky representation of C_0 (see Fig. SI3) does not provide a clear straight line and consequently this capacitance cannot be interpreted as a depletion capacitance. Indeed, the estimation of the width of the depletion region for this material ($N_A = 10^{17}$ cm^{-3}) [30] is approximately $w \approx 60$ nm at these potentials, indicating that the $CuGaO_2$ platelets must be fully depleted (the thickness of the platelets is around 5 nm as shown in Figure SI1). Alternatively, the origin of this capacitance could be chemical, and hence reflect the density of states of delafossite near the valence band. However, this possibility was ruled out due to the slow increase with potential, less than one order of magnitude in 500 mV and consequently the most reasonable origin for this capacitance is believed to result from the Helmholtz layer (10–100 μF cm^{-2}). On the other hand, after Mg doping, the Mott–Schottky representation of C_0 clearly shows that the origin of this capacitance is dielectric, with an acceptor density of $N_A = 9 \times 10^{19}$ cm^{-3}, and a flat band potential $V_{FB} = 0.23$ V vs Ag/Ag^+ (Fig. 4c). The estimation of the width of the depletion region $w = 6$ nm is consistent with this assignment, given the smallest dimension of these platelets (around 5 nm). On the other hand,

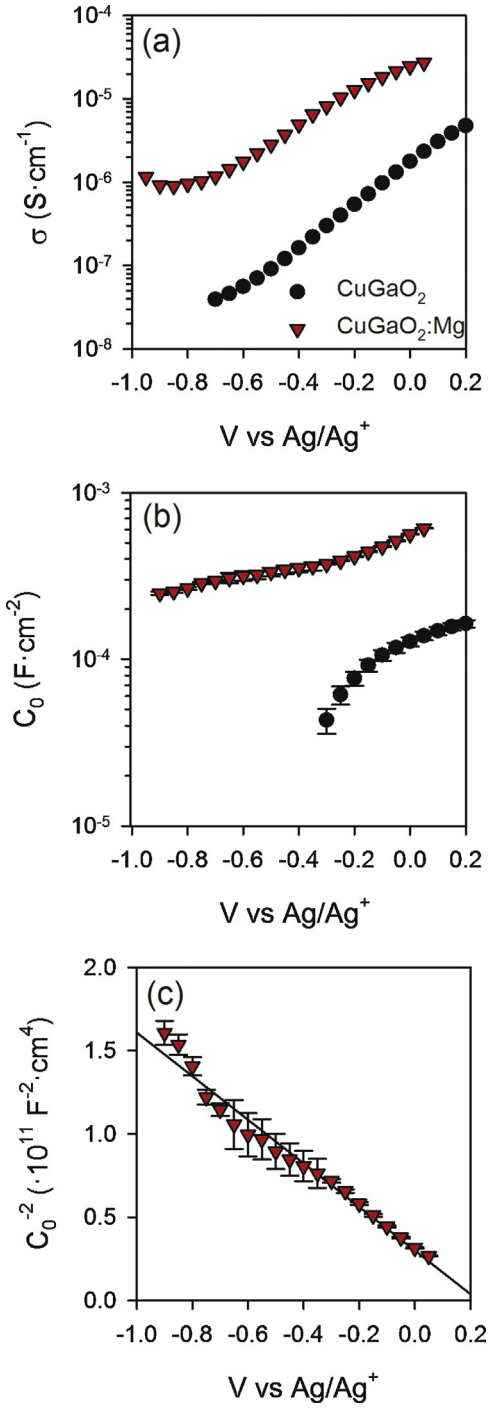

Fig. 4. (a) Conductivity (σ) and (b) capacitance (C_0) of undoped and Mg doped $CuGaO_2$ and (c) Mott–Schottky plot of the Mg doped material.

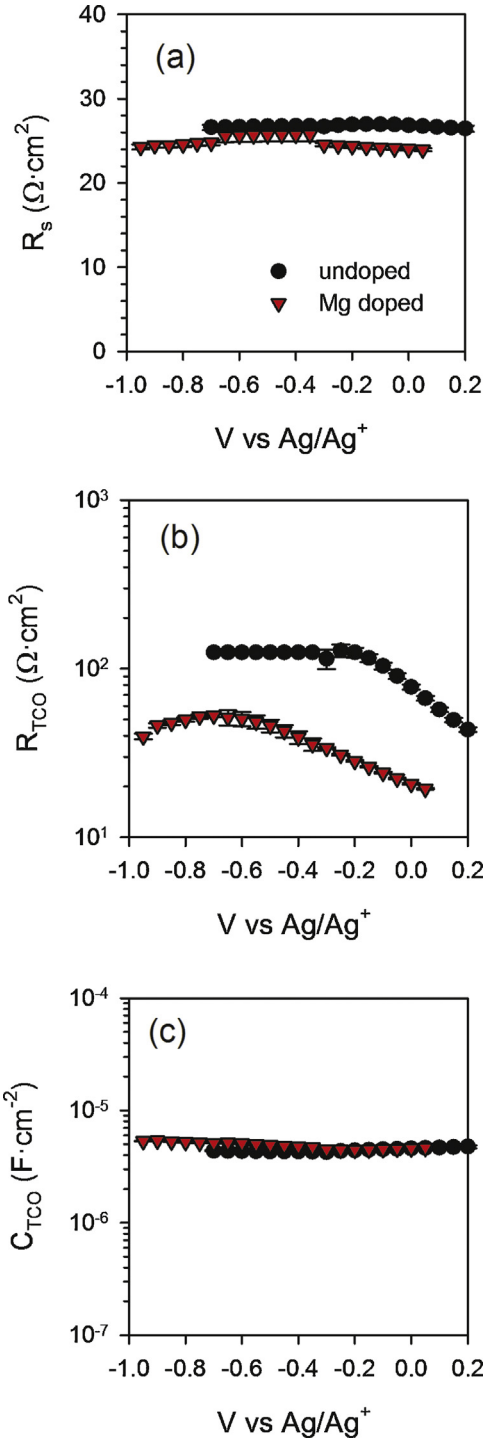

Fig. 5. (a) Series resistance, R_s (b) resistance at the FTO/$CuGaO_2$ interface, R_{TCO} and (c) capacitance at the FTO/solution interface (C_{TCO}) for both undoped and Mg doped $CuGaO_2$ materials after fitting the experimental impedance data to the physical model depicted in Fig. 3. Geometrical area of the samples: 0.25 cm^2.

C_{TCO}, the capacitance at the FTO/solution interface, systematically shows a constant value (C_{TCO} = 10 $\mu F\,cm^{-2}$) for both undoped and Mg doped materials through all the potential range evaluated, in good agreement with the double layer capacitance of FTO directly exposed to the electrolyte (not covered by $CuGaO_2$) [31].

Finally, the resistance at the contact FTO/$CuGaO_2$ (R_{TCO}) is higher for the undoped material, (approximately 100 $\Omega\,cm^{-2}$ vs 50 $\Omega\,cm^{-2}$ for the doped material) probably due to a better adhesion of the semiconductor nanoplatelets to the TCO substrate, while the series resistance, R_s is practically identical for both materials (20–30 $\Omega\,cm^{-2}$) (see Fig. 5).

4. Conclusions

The electrical properties of nanostructured $CuGaO_2$ films synthesized by a hydrothermal route have been evaluated using impedance spectroscopy methods. For the first time, hole conductivities for p-type nanostructured semiconductors could be estimated by using a transmission line approach. Conductivity of $CuGaO_2$ ranged 1–10 $\mu S\,cm^{-1}$ in the interval of applied bias tested and it increased one order of magnitude after Mg doping. On the

other hand, the measured capacitance corresponds to different mechanisms depending on the synthetic history. After Mg doping, the measured capacitance has a dielectric origin that reflects depletion of the semiconductor due to band bending. In these conditions, the estimated acceptor density is $N_A = 10^{19}\,cm^{-3}$ and the flat band potential, $V_{FB} = 0.23$ V vs Ag/Ag^+. On the other hand, without doping, the measured capacitance corresponds to the double layer capacitance, since the semiconductor is fully depleted at the testing conditions. The change of the conductivity and capacitance characteristics obtained demonstrates that the synthetic method used for the addition of Mg effectively dopes $CuGaO_2$. Additionally, this doping leads to a red-shift of 150 nm in the optical bandgap of $CuGaO_2$. We believe that the findings of this study clarifying the electrical characteristics of nanostructured $CuGaO_2$ films, will contribute to a better electrode design for photovoltaic and catalytic applications.

Acknowledgements

The research leading to these results is supported by Universitat Jaume I project P1 1B2011-50. The authors want to acknowledge Prof. Juan Bisquert for the enlightening discussions related to this manuscript.

Appendix A. Supplementary data

Supplementary data associated with this article can be found, in the online version, at http://dx.doi.org/10.1016/j.electacta.2013.09.129.

References

[1] L.M. Abrantes, L.M. Peter, Transient photocurrents at passive iron electrodes, J. Electroanal. Chem., Interfacial Electrochem. 150 (1983) 593.
[2] L. Tong, A. Iwase, A. Nattestad, U. Bach, M. Weidelener, G. Gotz, A. Mishra, P. Bäuerle, R. Amal, G.G. Wallace, A.J. Mozer, Sustained solar hydrogen generation using a dye-sensitised NiO photocathode/$BiVO_4$ tandem photo-electrochemical device, Energy Environ. Sci. 5 (2012) 9472–9475.
[3] J. Bandara, H. Weerasinghe, Solid-state dye-sensitized solar cell with p-type NiO as a hole collector, Sol. Energy Mater. Sol. Cells 85 (2005) 385–390.
[4] J.J. He, H. Lindstrom, A. Hagfeldt, S.E. Lindquist, Dye-sensitized nanostructured p-type nickel oxide film as a photocathode for a solar cell, J. Phys. Chem. B 103 (1999) 8940–8943.
[5] A. Nattestad, A.J. Mozer, M.K.R. Fischer, Y.B. Cheng, A. Mishra, P. Bauerle, U. Bach, Highly efficient photocathodes for dye-sensitized tandem solar cells, Nat. Mater. 9 (2010) 31–35.
[6] F. Odobel, L. Le Pleux, Y. Pellegrin, E. Blart, New photovoltaic devices based on the sensitization of p-type semiconductors: challenges and opportunities, Acc. Chem. Res. 43 (2010) 1063–1071.
[7] A. Kudo, Photocatalyst materials for water splitting, Catal. Surv. Asia 7 (2003) 31–38.
[8] T.K. Townsend, N.D. Browning, F.E. Osterloh, Nanoscale strontium titanate photocatalysts for overall water splitting, ACS Nano 6 (2012) 7420–7426.
[9] M.G. Walter, E.L. Warren, J.R. McKone, S.W. Boettcher, Q.X. Mi, E.A. Santori, N.S. Lewis, Solar water splitting cells, Chem. Rev. 110 (2010) 6446–6473.
[10] M. Hara, T. Kondo, M. Komoda, S. Ikeda, K. Shinohara, A. Tanaka, J.N. Kondo, K. Domen, Cu_2O as a photocatalyst for overall water splitting under visible light irradiation, Chem. Commun. (1998) 357–358.
[11] A. Paracchino, J.C. Brauer, J.E. Moser, E. Thimsen, M. Graetzel, Synthesis characterization of high-photoactivity electrodeposited Cu_2O solar absorber by photoelectrochemistry and ultrafast spectroscopy, J. Phys. Chem. C 116 (2012) 7341–7350.
[12] A. Paracchino, N. Mathews, T. Hisatomi, M. Stefik, S.D. Tilley, M. Gratzel, Ultrathin films on copper(I) oxide water splitting photocathodes: a study on performance and stability, Energy Environ. Sci. 5 (2012) 8673–8681.
[13] A. Paracchino, V. Laporte, K. Sivula, M. Gratzel, E. Thimsen, Highly active oxide photocathode for photoelectrochemical water reduction, Nat. Mater. 10 (2011) 456–461.
[14] G.K. Mor, O.K. Varghese, R.H.T. Wilke, S. Sharma, K. Shankar, T.J. Latempa, K.S. Choi, C.G. Grimes, p-Type Cu–Ti–O nanotube arrays and their use in self-biased heterojunction photoelectrochemical diodes for hydrogen generation, Nano Lett. 8 (2008) 1906–1911.
[15] K. Ueda, T. Hase, H. Yanagi, H. Kawazoe, H. Hosono, H. Ohta, M. Orita, M. Hirano, Epitaxial growth of transparent p-type conducting $CuGaO_2$ thin films on sapphire (0 0 1) substrates by pulsed laser deposition, J. Appl. Phys. 89 (2001) 1790–1793.
[16] R. Srinivasan, B. Chavillon, C. Doussier-Brochard, L. Cario, M. Paris, E. Gautron, P. Deniard, F. Odobel, S. Jobic, Tuning the size and color of the p-type wide band gap delafossite semiconductor $CuGaO_2$ with ethylene glycol assisted hydrothermal synthesis, J. Mater. Chem. 18 (2008) 5647–5653.
[17] A. Renaud, B. Chavillon, L. Le Pleux, Y. Pellegrin, E. Blart, A. Boujtita, T. Pauport, L. Cario, S. Jobic, F. Odobel, $CuGaO_2$: a promising alternative for NiO in p-type dye solar cells, J. Mater. Chem. 22 (2012) 14353–14356.
[18] M. Yu, G. Natu, Z. Ji, Y. Wu, p-Type dye-sensitized solar cells based on delafossite $CuGaO_2$ nanoplates with saturation photovoltages exceeding 460 mV, J. Phys. Chem. Lett. 3 (2012) 1074–1078.
[19] J.W. Lekse, M.K. Underwood, J.P. Lewis, C. Matranga, Synthesis characterization electronic structure, and photocatalytic behavior of $CuGaO_2$ and $CuGa1\text{-}xFexO_2$ ($x = 0.05, 0.10, 0.15, 0.20$) delafossites, J. Phys. Chem. C 116 (2012) 1865–1872.
[20] F. Fabregat-Santiago, G. Garcia-Belmonte, I. Mora-Sero, J. Bisquert, Characterization of nanostructured hybrid and organic solar cells by impedance spectroscopy, Phys. Chem. Chem. Phys. 13 (2011) 9083–9118.
[21] R. Srinivasan, B. Chavillon, C. Doussier-Brochard, L. Cario, M. Paris, E. Gautron, P. Deniard, F. Odobel, S. Jobic, Tuning the size and color of the p-type wide band gap delafossite semiconductor CuGaO(2) with ethylene glycol assisted hydrothermal synthesis, J. Mater. Chem. 18 (2008) 5647–5653.
[22] Z.B. Chen, T.F. Jaramillo, T.G. Deutsch, A. Kleiman-Shwarsctein, A.J. Forman, N. Gaillard, R. Garland, K. Takanabe, C. Heske, M. Sunkara, E.W. McFarland, K. Domen, E.L. Miller, J.A. Turner, H.N. Dinh, Accelerating materials development for photoelectrochemical hydrogen production: standards for methods, definitions, and reporting protocols, J. Mater. Res. 2 (5) (2010) 3–16.
[23] F.A. Benko, F.P. Koffyberg, Optoelectronic properties of para-type and normal-type delafossite $CuFeO_2$, J. Phys. Chem. Solids 48 (1987) 431–434.
[24] X. Nie, S.-H. Wei, S.B. Zhang, Bipolar doping and band-gap anomalies in delafossite transparent conductive oxides, Phys. Rev. Lett. 88 (2002), 066405–066401–066404.
[25] J. Bisquert, Theory of the impedance of electron diffusion and recombination in a thin layer, J. Phys. Chem. B 106 (2002) 325–333.
[26] J. Bisquert, Chemical capacitance of nanostructured semiconductors: its origin and significance for nanocomposite solar cells, Phys. Chem. Chem. Phys. 5 (2003) 5360–5364.
[27] S. Gimenez, H.K. Dunn, P. Rodenas, F. Fabregat-Santiago, S.G. Miralles, E.M. Barea, R. Trevisan, A. Guerrero, J. Bisquert, Carrier density and interfacial kinetics of mesoporous TiO_2 in aqueous electrolyte determined by impedance spectroscopy, J. Electroanal. Chem. 668 (2012) 119–125.
[28] G. Garcia-Belmonte, J. Bisquert, Impedance analysis of galvanostatically synthesized polypyrrole films. Correlation of ionic diffusion and capacitance parameters with the electrode morphology, Electrochim. Acta 47 (2002) 4263–4272.
[29] J. Tate, M.K. Jayaraj, A.D. Draeseke, T. Ulbrich, A.W. Sleight, K.A. Vanaja, R. Nagarajan, J.F. Wager, R.L. Hoffman, p-Type oxides for use in transparent diodes, Thin Solid Films 411 (2002) 119–124.
[30] I. Hamadaa, H. Katayama-Yoshida, Energetics of native defects in $CuAlO_2$, Phys. B 376–377 (2006) 808–8011.
[31] F. Fabregat-Santiago, G. Garcia-Belmonte, J. Bisquert, P. Bogdanoff, A. Zaban, Mott–Schottky analysis of nanoporous semiconductor electrodes in dielectric state deposited on $SnO_2(F)$ conducting substrates, J. Electrochem. Soc. 150 (2003) E293–E298.